

Excited-state population distributions of alkaline-earth metal in a hollow cathode lamp

Pengyuan Chang (常鹏媛), Bo Pang (逢博), Yisheng Wu (吴一胜),
and Jingbiao Chen (陈景标)*

State Key Laboratory of Advanced Optical Communication System and Network, School of Electronics
Engineering and Computer Science, Peking University, Beijing 100871, China

*Corresponding author: jbchen@pku.edu.cn

Received October 22, 2017; accepted January 4, 2018; posted online March 7, 2018

The intensities of fluorescence spectral lines of Ca atoms and Sr atoms in two different hollow cathode lamps (HCLs) are measured by element-balance-detection technology. In the wavelength range of 350–750 nm in the visible spectral region, using the individual strongest line (Ca 422.67 nm, Sr 460.73 nm) as the bench mark, the population ratios between the excited states of Ca atoms and Sr atoms are calculated by rate equations and the spontaneous transition probabilities. The HCLs with populations at excited states can be used to realize the frequency stabilization reference of the laser frequency standard.

OCIS codes: 300.6210, 020.1335, 260.2510.

doi: 10.3788/COL201816.033001.

Hollow cathode lamps (HCLs) with alkaline-earth metal are attracting growing attention nowadays as sources of intense atomic spectral lines in various physical devices applied in atomic absorption and emission spectroscopy^[1–3]. Furthermore, the atom unit most frequently employed in a traditional Faraday anomalous dispersion optical filter (FADOF)^[4] is a vapor cell with atomic density determined by thermal equilibrium^[5–8]. Hence, the samples of atomic filters have to be heated to high temperatures to get an atomic density high enough to guarantee the transmittance^[9,10]. To overcome this limitation, an innovative method of utilizing an HCL to realize a Sr element FADOF was proposed, as the HCLs can provide the high atomic density at room temperature^[11]. Moreover, since the state-of-the-art HCLs cover about 70 kinds of high melting point metal elements, we believe that, due to its rich spectral lines, without heating, scalability, low fabrication cost, and potential applications in various atomic spectra^[12–16] they can be used in submarine communication systems as well as excited-state FADOFs without the use of a pump laser^[5,6].

Basic knowledge about HCLs is meaningful for the exploration of further applications^[17,18]. The HCLs have rich atomic spectral lines; nevertheless, the spectral measurements are often contaminated by buffer gas-line interference^[14–23]. A new method of measurement, as shown in Fig. 1, element-balance-detection technology, is introduced by us, which can remove the effect of the buffer gas-line via the subtraction relation between two spectral signals of Ca HCL and Sr HCL, as shown in Figs. 2 and 3. This method is simply described as follows: two spectral signals of Ca HCL and Sr HCL both include the buffer gas-line; in order to distinguish the atom lines between the spectral signals, we conduct a subtraction operation of two signals to make the buffer gas-lines offset each other. Although the components of the buffer gas may

be different, the results imply that the subtraction procedure is coping better with this problem. Hence, the element-balance-detection technology is applicable for similar situations in atomic spectroscopy measurement, which exists in the interference of impurity lines.

In this Letter, we measured the intensities of fluorescence spectral lines of Ca and Sr atoms in two different HCLs, respectively. In the wavelength range of 350–750 nm in the visible spectral region, using the individual strongest line (Ca 422.67 nm, Sr 460.73 nm) as the bench mark, we calculated the population ratios between the excited states by rate equations and spontaneous transition probabilities. The measured results showed that the intensities of the spectral lines of Ca and Sr atoms are significantly different.

The measurement setup is schematically shown in Fig. 1. Figure 2 shows the energy diagrams of the transitions related to the Ca and Sr atoms' spectral signal. The Sr HCL and Ca HCL are powered by Power1 and Power2 (generating a current range of 0 to 20 mA), respectively, which are placed across the cathode and anode terminals. The intensities of the fluorescence spectral lines of Ca and Sr atoms were strikingly different along with the current increase. The USB2000+ spectrometer in connection with

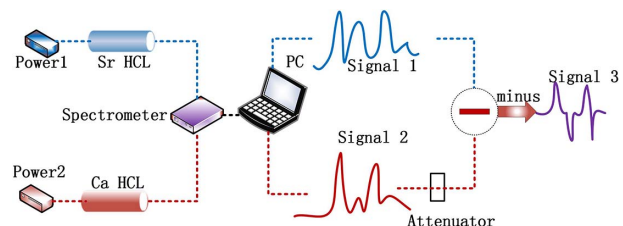


Fig. 1. Experimental schemes of Ca HCL and Sr HCL in the configuration of element-balance-detection technology for spectrum research.

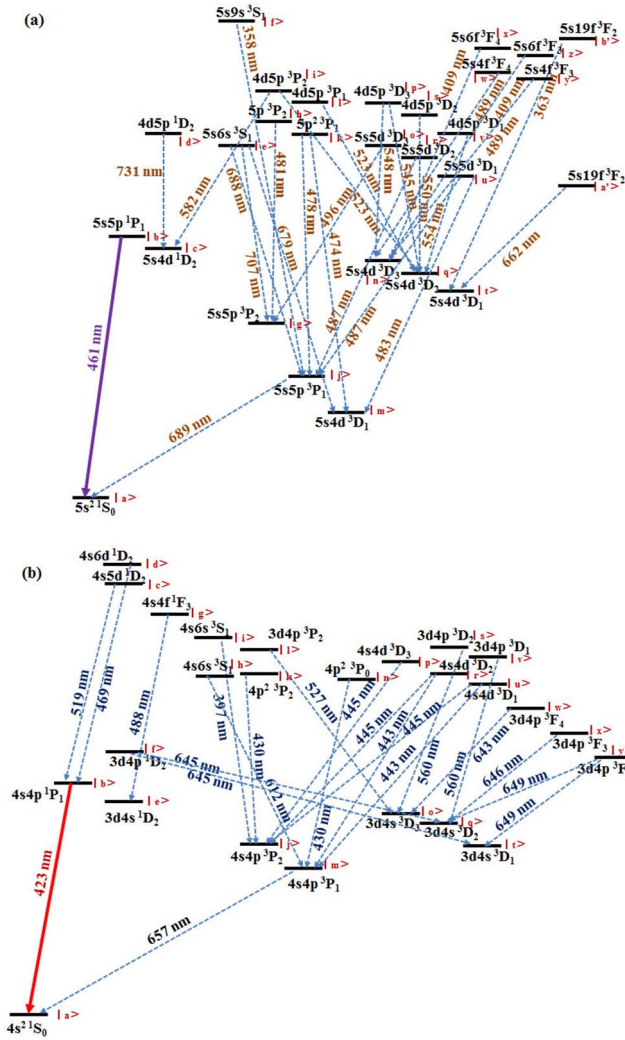


Fig. 2. (a) Energy diagram of Sr atoms' transitions. (b) Energy diagram of Ca atoms' transitions.

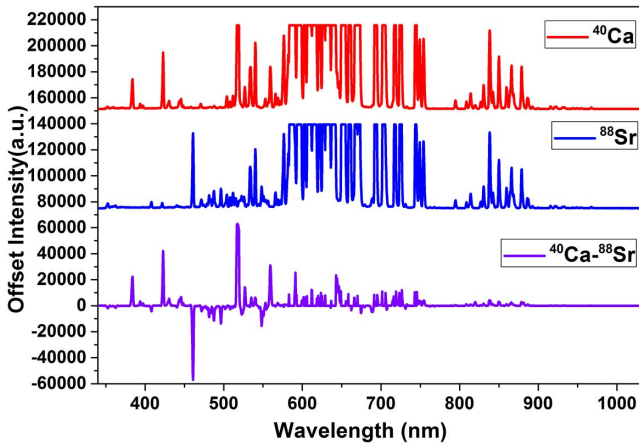


Fig. 3. Measured spectral intensities of Ca HCL (red line), Sr HCL (blue line), and the element-balance-detection signal with little effect of the buffer gas-lines (purple line).

a personal computer (PC) produced by Ocean Optics Company in USA with a resolution of 1.5 nm is used to measure the fluorescence spectra. One path is Ca HCL

spectral signal 1, and the other path is Sr HCL spectral signal 2. Since the spectrometer has only one channel, signals 1 and 2 were not measured simultaneously. The measured signals can be adjusted by a suitable attenuator (coefficient), which is an appropriate constant coefficient, to adjust the amplitude when processing the data. The measured spectral signals are shown in Fig. 3.

When the distance of the spectrometer from the HCLs is set appropriately, the current of Power1 and Power2 is set to be 17 and 20 mA, respectively. The relative intensities of the spectral lines of Ca atoms and Sr atoms can be detected, as shown in Fig. 3. In order to display the signal clearly, it is divided into four pictures according to the wavelength ranges, as shown in Fig. 4. The wavelength ranges of Figs. 4(a), 4(b), 4(c), and 4(d) are 340–440, 440–540, 540–640, and 640–740 nm, respectively.

By reference to the NIST atomic spectra database^[24], the spontaneous transition probabilities $A_{\mu\eta}$ and the wavelengths involved in the calculation are listed in Table 1 (Ca) and Table 2 (Sr). Data in columns 1–4 are wavelengths, spectral signal intensities, spontaneous transition probabilities, and transition level, respectively.

The intensities of the atomic lines depend on the number of sputtered metal atoms, which depends on the kinetic energy of the buffer gas ions, which, in turn, is dictated by the lamp current.

The intensity (P) of the transition signal between two energy levels can be expressed as $P_{\lambda} = n_{\mu} A_{\mu\eta} h\nu_{\lambda}$, where λ is the transition wavelength, n_{μ} is the atomic density in the level numbered μ ($\mu = a, b, c, \dots$), $A_{\mu\eta}$ is the spontaneous transition probability between the μ and η energy levels, ν is the transition frequency, and h is the Planck constant^[22,25,26]. The Ca atoms' transition signal intensity studied can be clearly expressed with Eqs. (1)–(13). The Sr atoms' transition signal intensity studied can be clearly expressed with Eqs. (14)–(36):

$$P_{397} = n_i A_{ij} h\nu_{397}, \quad (1)$$

$$P_{423} = n_b A_{ba} h\nu_{423}, \quad (2)$$

$$P_{430} = n_k A_{kj} h\nu_{430,1} + n_n A_{nm} h\nu_{430,2}, \quad (3)$$

$$P_{443} = n_r A_{rm} h\nu_{443,1} + n_u A_{um} h\nu_{443,2}, \quad (4)$$

$$P_{445} = n_p A_{pj} h\nu_{445,1} + n_r A_{rj} h\nu_{445,2} + n_u A_{uj} h\nu_{445,3}, \quad (5)$$

$$P_{519} = n_c A_{cb} h\nu_{519}, \quad (6)$$

$$P_{527} = n_l A_{lo} h\nu_{527}, \quad (7)$$

$$P_{560} = n_s A_{so} h\nu_{560,1} + n_v A_{vq} h\nu_{560,2}, \quad (8)$$

$$P_{612} = n_h A_{hm} h\nu_{612}, \quad (9)$$

$$P_{643} = n_w A_{wo} h\nu_{643}, \quad (10)$$

$$P_{645} = n_f A_{fq} h\nu_{645,1} + n_f A_{ft} h\nu_{645,2}, \quad (11)$$

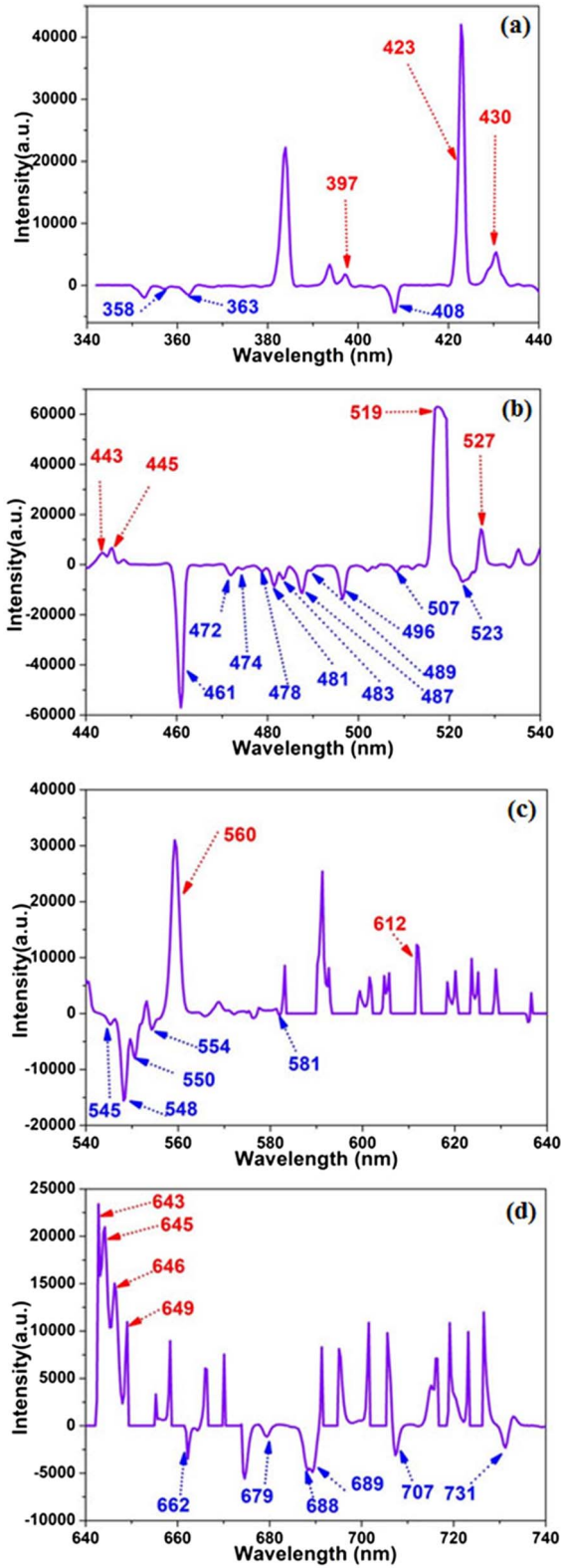


Fig. 4. (a) Intensities of 397, 423, 430 nm of Ca atoms and 358, 363, 408 nm of Sr atoms. (b) The intensities of 443, 445, 519, 527 nm of Ca atoms and 461, 474, 478, 481, 483, 487, 489, 496, 523 nm of Sr atoms. (c) The intensities of 560, 612 nm of Ca atoms and 545, 548, 550, 554, 581 nm of Sr atoms. (d) The intensities of 643, 645, 646, 649 nm of Ca atoms and 662, 679, 688, 689, 707, 731 nm of Sr atoms.

Table 1. Wavelengths, Spectral Signal Relative Intensities, Spontaneous Transition Probabilities, and Transition levels of Ca Atoms^a

λ (nm)	I (a.u.)	$A_{\mu\eta}/10^6 \text{ s}^{-1}$	Transition Level
397.3708	1805	17.5	$4s6s \ ^3S_1 \rightarrow 4s4p \ ^3P_2$
422.6728	42005	218	$4s4p \ ^1P_1 \rightarrow 4s^2 \ ^1S_0$
430.2528	5365	136	$4p^2 \ ^3P_2 \rightarrow 4s4p \ ^3P_2$
430.7744		199	$4p^2 \ ^3P_0 \rightarrow 4s4p \ ^3P_1$
443.4957	4714	67	$4s4d \ ^3D_2 \rightarrow 4s4p \ ^3P_1$
443.5679		34.2	$4s4d \ ^3D_1 \rightarrow 4s4p \ ^3P_1$
445.4779	6688	87	$4s4d \ ^3D_3 \rightarrow 4s4p \ ^3P_2$
445.5887		20	$4s4d \ ^3D_2 \rightarrow 4s4p \ ^3P_2$
445.6616		2.45	$4s4d \ ^3D_1 \rightarrow 4s4p \ ^3P_2$
518.8844	60836	40	$4s5d \ ^1D_2 \rightarrow 4s4p \ ^1P_1$
527.0270	14172	50	$3d4p \ ^3P_2 \rightarrow 3d4s \ ^3D_3$
560.1277	31001	8.6	$3d4p \ ^3D_2 \rightarrow 3d4s \ ^3D_3$
560.2842		14	$3d4p \ ^3D_1 \rightarrow 3d4s \ ^3D_2$
612.2217	12301	28.7	$4s5s \ ^3S_1 \rightarrow 4s4p \ ^3P_2$
643.9075	20413	53	$3d4p \ ^3F_4 \rightarrow 3d4s \ ^3D_3$
644.9808	17355	9	$3d4p \ ^1D_2 \rightarrow 3d4s \ ^3D_1$
645.5598	15043	1.4	$3d4p \ ^1D_2 \rightarrow 3d4s \ ^3D_2$
646.2567		47	$3d4p \ ^3F_3 \rightarrow 3d4s \ ^3D_2$
649.3781	10966	44	$3d4p \ ^3F_2 \rightarrow 3d4s \ ^3D_1$
649.9650		8.1	$3d4p \ ^3F_2 \rightarrow 3d4s \ ^3D_2$

^aBy reference to NIST atomic spectra database.

$$P_{646} = n_x A_{xq} h\nu_{646}, \quad (12)$$

$$P_{649} = n_y A_{yt} h\nu_{649,1} + n_y A_{yq} h\nu_{649,2}, \quad (13)$$

$$P_{358} = n_f A_{fj} h\nu_{358}, \quad (14)$$

$$P_{363} = n_{b'a} A_{b'a} h\nu_{363}, \quad (15)$$

$$P_{409} = n_x A_{xn} h\nu_{409,1} + n_y A_{yn} h\nu_{409,2}, \quad (16)$$

$$P_{461} = n_b A_{ba} h\nu_{461}, \quad (17)$$

$$P_{474} = n_k A_{km} h\nu_{474}, \quad (18)$$

$$P_{478} = n_k A_{kj} h\nu_{478}, \quad (19)$$

$$P_{481} = n_h A_{hg} h\nu_{481}, \quad (20)$$

$$P_{483} = n_u A_{um} h\nu_{483}, \quad (21)$$

$$P_{487} = n_r A_{rj} h\nu_{487,1} + n_u A_{uj} h\nu_{487,2}, \quad (22)$$

$$P_{489} = n_z A_{zn} h\nu_{489,1} + n_y A_{yn} h\nu_{489,2}, \quad (23)$$

Table 2. Wavelengths, Spectral Signal Relative Intensities, Spontaneous Transition Probabilities, and Transition Levels of Sr Atoms^a

λ (nm)	I (a.u.)	$A_{\mu\nu}/10^6 \text{ s}^{-1}$	Transition Level
357.7243	519	A_{fj}	5s9s $^3S_1 \rightarrow 5s5p \ ^3P_1$
362.9144	1534	$A_{b't}$	5s7d $^3D_1 \rightarrow 5s5p \ ^3P_0$
408.7344	4326	A_{xn}	5s6f $^3F_4 \rightarrow 5s4d \ ^3D_3$
408.7442		A_{yn}	5s6f $^3F_3 \rightarrow 5s4d \ ^3D_3$
460.7331	57023	201	5s5p $^1P_1 \rightarrow 5s^2 \ ^1S_0$
474.1922	1818	39	5p $^2 \ ^3P_1 \rightarrow 5s5p \ ^3P_0$
478.43198	2641	30	5p $^2 \ ^3P_1 \rightarrow 5s5p \ ^3P_1$
481.18799	8708	90	5p $^2 \ ^3P_2 \rightarrow 5s5p \ ^3P_2$
483.20425	5721	33	5s5d $^3D_1 \rightarrow 5s5p \ ^3P_0$
487.2490	11350	48	5s5d $^3D_2 \rightarrow 5s5p \ ^3P_1$
487.60745		26.3	5s5d $^3D_1 \rightarrow 5s5p \ ^3P_1$
489.19800	2426	38	5s4f $^3F_4 \rightarrow 5s4d \ ^3D_3$
489.26420		4.3	5s4f $^3F_3 \rightarrow 5s4d \ ^3D_3$
496.22630	13730	61.4	5s5d $^3D_3 \rightarrow 5s5p \ ^3P_2$
522.92679	6872	22.7	4d5p $^3P_2 \rightarrow 5s4d \ ^3D_2$
523.85479		73	4d5p $^3P_1 \rightarrow 5s4d \ ^3D_2$
545.08373	1996	14.7	4d5p $^3D_3 \rightarrow 5s4d \ ^3D_2$
548.08638	15568	79	4d5p $^3D_3 \rightarrow 5s4d \ ^3D_3$
550.4181	8059	54	4d5p $^3D_2 \rightarrow 5s4d \ ^3D_2$
554.0050	2902	28.4	4d5p $^3D_1 \rightarrow 5s4d \ ^3D_2$
581.67702	329	0.3	4d5p $^3P_2 \rightarrow 5s4d \ ^1D_2$
661.72651	3486	16	4d5p $^3F_2 \rightarrow 5s4d \ ^3D_1$
679.10198	1157	8.9	5s6s $^3S_1 \rightarrow 5s5p \ ^3P_0$
687.83128	4723	27	5s6s $^3S_1 \rightarrow 5s5p \ ^3P_1$
689.25894	4894	0.0469	5s5p $^3P_1 \rightarrow 5s^2 \ ^1S_0$
707.0072	3107	42	5s6s $^3S_1 \rightarrow 5s5p \ ^3P_2$
730.94166	2318	39	4d5p $^1D_2 \rightarrow 5s4d \ ^1D_2$

^aBy reference to NIST atomic spectra database.

$$P_{496} = n_o A_{og} h\nu_{496}, \quad (24)$$

$$P_{523} = n_l A_{lq} h\nu_{523,1} + n_i A_{iq} h\nu_{523,2}, \quad (25)$$

$$P_{545} = n_p A_{pq} h\nu_{545}, \quad (26)$$

$$P_{548} = n_p A_{pn} h\nu_{548}, \quad (27)$$

$$P_{550} = n_s A_{sq} h\nu_{550}, \quad (28)$$

$$P_{554} = n_v A_{vq} h\nu_{554}, \quad (29)$$

$$P_{581} = n_i A_{ic} h\nu_{582}, \quad (30)$$

$$P_{662} = n_{d'} A_{d't} h\nu_{662}, \quad (31)$$

$$P_{679} = n_e A_{em} h\nu_{679}, \quad (32)$$

$$P_{688} = n_e A_{ej} h\nu_{688}, \quad (33)$$

$$P_{689} = n_j A_{ja} h\nu_{689}, \quad (34)$$

$$P_{707} = n_e A_{eg} h\nu_{707}, \quad (35)$$

$$P_{731} = n_d A_{dc} h\nu_{731}. \quad (36)$$

From Eqs. (1)–(13), the 423 nm transition of Ca atoms has only one spectral line corresponding to the transition, 4s4p $^1P_1 \rightarrow 4s^2 \ ^1S_0$. Given that the population at the $|b\rangle$ energy level is the maximum, the value of n_b is used as the bench mark to calculate the results of n_μ/n_b . The calculated results of n_μ/n_b of Ca atoms are shown in Table 3. Because the number of unknowns is larger than the number of equations, we finally get several sets of algebraic results; those are the results obtained in the bottom lines in Table 3.

From Eqs. (14)–(36), the 461 nm transition of Sr atoms also has only one spectral line corresponding to the transition, 5s5p $^1P_1 \rightarrow 5s^2 \ ^1S_0$. Given that the population at the $|b\rangle$ energy level is the maximum, the value of n_b is used as the bench mark to calculate the results of

Table 3. Sr HCL and Ca HCL Calculation Results of n_μ/n_η

n_μ/n_b (Sr)	Value (Sr)	n_μ/n_b (Ca)	Value (Ca)
n_k/n_b	0.69	n_i/n_b	0.50
n_h/n_b	0.35	n_c/n_b	9.70
n_u/n_b	0.64	n_l/n_b	1.83
n_o/n_b	0.85	n_h/n_b	3.24
n_p/n_b	0.70	n_w/n_b	3.04
n_s/n_b	0.62	n_x/n_b	2.54
n_v/n_b	0.43	n_y/n_b	1.68
n_i/n_b	5.03	$(2n_k + 3n_y)/n_b$	0.36
$n_{d'}/n_b$	1.11	$(4n_p + n_r)/n_b$	1.84
n_e/n_b	0.68	$(2n_s + 3n_v)/n_b$	49.64
n_j/n_b	550.29	n_f/n_b	13.21
n_d/n_b	0.33		
$(2n_r + n_u)/n_b$	1.61		
$(9n_z + n_y)/n_b$	2.14		
$(n_i + 3n_l)/n_b$	1.21		
$(A_{fj}n_f)/n_b$	1.42		
$(A_{b't}n_{b'})/n_b$	3.76		
$(A_{xn}n_x + A_{yn}n_y)/n_b$	13.54		

n_μ/n_b . The calculated results of n_μ/n_b of Sr atoms are shown in Table 3. By reference to the NIST atomic spectra database^[24], because of the absence of the spontaneous transition probability between the corresponding energy levels A_{fj} , $A_{j't}$, A_{xn} , and A_{yn} , we can only use the symbols to calculate the equations and display the results.

As shown in Table 3, the populations at the other energy levels are also very large. However, due to the wavelength spacing of 1 nm between 643, 645, and 646 nm, the overlap of signals and the relative lower resolution of 1.5 nm of the spectrometer may bring measurement errors. But, this problem can be solved by using a high-resolution spectrometer. In addition, because the measurable range of the spectrometer, 400–1000 nm, did not cover all the lines of Ca and Sr atoms, some higher excited states may not be considered. Hence, the calculated population ratios have the errors ± 0.25 . Since the state-of-the-art commercial HCLs cover about 70 kinds of high melting point metal elements and can excite large amounts of levels of neutral atoms, they thus provide abundant transitions for frequency standard fields, etc.^[27–31]

In conclusion, population ratios between the excited states according to the spontaneous transition probabilities with rate equations and the measured intensities of fluorescence spectral lines of Ca atoms and Sr atoms in HCL within the visible spectral region from 350 to 750 nm are calculated; the population density of the energy level is also obtained. Sufficient populations at the excited states are found when the HCLs are lit. The HCLs with populations at excited states can be used to realize the frequency stabilization reference of the laser frequency standard^[12,23,32–40].

This work was supported by the National Natural Science Foundation of China (No. 91436210).

References

1. A. F. Lagalante, *Appl. Spectrosc. Rev.* **34**, 173 (1999).
2. N. H. Bings, A. Bogaerts, and J. A. C. Broekaert, *Anal. Chem.* **76**, 3313 (2004).
3. F. Wang, F. Zhao, F. Qi, H. Wu, D. Zhong, and G. Mei, *Spectrosc. Spect. Anal.* **29**, 1164 (2009) (in Chinese).
4. Y. Ohman, *Stock. Obs. Ann.* **19**, 9 (1956).
5. Q. Sun, W. Zhuang, Z. Liu, and J. Chen, *Opt. Lett.* **36**, 4611 (2011).
6. P. Chang, T. Shi, S. Zhang, H. Shang, D. Pan, and J. Chen, *Chin. Opt. Lett.* **15**, 121401 (2017).
7. L. Ling and G. Bi, *Opt. Lett.* **39**, 3324 (2014).
8. S. Liang, Y. Xu, and Y. Q. Lin, *Chin. Opt. Lett.* **15**, 090201 (2017).
9. Z. Tao, Y. Hong, B. Luo, J. Chen, and H. Guo, *Opt. Lett.* **40**, 4348 (2015).
10. P. Chang, H. Peng, S. Zhang, Z. Chen, B. Luo, J. Chen, and H. Guo, *Sci. Rep.* **7**, 8995 (2017).
11. D. Pan, X. Xue, H. Shang, B. Luo, J. Chen, and H. Guo, *Sci. Rep.* **6**, 29882 (2016).
12. J. Chen, *Chin. Sci. Bull.* **54**, 348 (2009).
13. W. Zhuang, Y. Hong, Z. Gao, C. Zhu, and J. Chen, *Chin. Opt. Lett.* **12**, 60 (2014).
14. U. Dammalapati, I. Norris, and E. Riis, *J. Phys. B At. Mol. Opt. Phys.* **42**, 165001 (2009).
15. S. Zhu, T. Chen, X. Li, and Y. Wang, *J. Opt. Soc. Am. B* **31**, 2302 (2014).
16. T. Chen, C. Lin, J. Shy, and Y. Liu, *J. Opt. Soc. Am. B* **30**, 2966 (2013).
17. S. Xu, Z. Yang, G. Wang, S. Dai, L. Hu, and Z. Jiang, *Chin. Opt. Lett.* **385**, 544 (2003).
18. S. Huo, Z. Zhang, Z. Wu, H. Zheng, T. Liu, X. Xue, J. Song, and Y. Zhang, *Chin. Opt. Lett.* **9**, 121902 (2011).
19. Z. Tao, Y. Wang, S. Zhang, D. Wang, Y. Hong, W. Zhuang, and J. Chen, *Chin. Opt. Lett.* **11**, 100202 (2013).
20. Z. Tao, Y. Wang, Y. Hong, D. Wang, S. Zhang, W. Zhuang, and J. Chen, *Chin. Sci. Bull.* **58**, 1876 (2013).
21. Y. Wu and J. Chen, "A research on the population of the atoms in hollow cathode lamp," Master Dissertation (Peking University, 2017).
22. Q. Sun, X. Miao, R. Sheng, and J. Chen, *Chin. Phys. B* **21**, 033201 (2012).
23. F. Riehle, *Frequency Standards* (Wiley VCH, 2004).
24. <http://physics.nist.gov/cgi-bin/ASD/lines/>.
25. O. S. Heavens, *J. Opt. Soc. Am.* **51**, 1058 (1961).
26. M. S. Safronova, C. J. Williams, and C. W. Clark, *Phys. Rev. A* **69**, 022509 (2004).
27. Y. Wang, *Chin. Sci. Bull.* **54**, 347 (2009).
28. Q. Wang, Y. Lin, F. Meng, Y. Li, B. Lin, E. Zang, T. Li, and Z. Fang, *Chin. Phys. B* **33**, 45 (2016).
29. Y. Yao, Y. Jiang, L. Wu, H. Yu, Z. Bi, and L. Ma, *Appl. Phys. Lett.* **109**, 131102 (2016).
30. Z. Wang, X. Lv, and J. Chen, *Chin. Opt. Lett.* **9**, 041402 (2011).
31. Z. Zheng, W. Fan, and B. Xue, *Chin. Opt. Lett.* **9**, S10506 (2011).
32. Y. Cheng, J. Jiang, and J. Mitroy, *Phys. Rev. A* **88**, 022511 (2013).
33. T. Akatsuka, K. Tanihara, K. Komito, K. Ooi, and A. Morinaga, *Phys. Rev. A* **86**, 023418 (2012).
34. Y. Long, Z. Xiong, X. Zhang, M. Zhang, B. Lu, and L. He, *Chin. Opt. Lett.* **12**, 021401 (2014).
35. S. Qiao, Y. Zhang, X. Shi, B. Jiang, L. Zhang, X. Cheng, L. Li, J. Wang, and L. Gui, *Chin. Opt. Lett.* **13**, 051602 (2015).
36. J. Zhang, J. Shi, S. Zuo, F. Liu, J. Bai, and J. Luo, *Chin. Opt. Lett.* **13**, 071002 (2015).
37. Q. Zhou, P. Chang, Z. Liu, X. Zhang, C. Zhu, and J. Chen, *Chin. Phys. Lett.* **34**, 034208 (2017).
38. J. Liu and K. Zhu, *Photon. Res.* **5**, 450 (2017).
39. Y. Luo, S. Yan, A. Jia, C. Wei, Z. Li, E. Wang, and J. Yang, *Chin. Opt. Lett.* **14**, 121401 (2016).
40. Y. Guo, H. Lu, Q. Yin, and J. Su, *Chin. Opt. Lett.* **15**, 021402 (2017).